nature biotechnology

Cell type–specific delivery of siRNAs with aptamer-siRNA chimeras

James O McNamara II[1,3], Eran R Andrechek[2,3], Yong Wang[1], Kristi D Viles[1], Rachel E Rempel[2], Eli Gilboa[1], Bruce A Sullenger[1] & Paloma H Giangrande[1]

Technologies that mediate targeted delivery of small interfering RNAs (siRNAs) are needed to improve their therapeutic efficacy and safety. Therefore, we have developed aptamer-siRNA chimeric RNAs capable of cell type–specific binding and delivery of functional siRNAs into cells. The aptamer portion of the chimeras mediates binding to PSMA, a cell-surface receptor overexpressed in prostate cancer cells and tumor vascular endothelium, whereas the siRNA portion targets the expression of survival genes. When applied to cells expressing PSMA, these RNAs are internalized and processed by Dicer, resulting in depletion of the siRNA target proteins and cell death. In contrast, the chimeras do not bind to or function in cells that do not express PSMA. These reagents also specifically inhibit tumor growth and mediate tumor regression in a xenograft model of prostate cancer. These studies demonstrate an approach for targeted delivery of siRNAs with numerous potential applications, including cancer therapeutics.

First described in *Caenorhabditis elegans*, RNA interference (RNAi) is a cellular mechanism by which 21- to 23-nucleotide RNA duplexes trigger the degradation of cognate mRNAs[1]. The promise of RNAi-based therapeutic applications has been apparent since the demonstration that exogenous small interfering RNAs (siRNAs) can silence gene expression via the RNAi pathway in mammalian cells[2]. The properties of RNAi that are attractive for therapeutics include (i) stringent target-gene specificity, (ii) relatively low immunogenicity of siRNAs and (iii) simplicity of design and testing of siRNAs.

A critical technical hurdle for RNAi-based clinical applications is the delivery of siRNAs across the plasma membrane of cells *in vivo*. A number of solutions for this problem have been described, including cationic lipids[3], viral vectors[4–6], high-pressure injection[7] and modifications of the siRNAs (e.g., chemical, lipid, steroid, protein)[8–13]. However, most of the approaches described to date have the disadvantage of delivering siRNAs to cells nonspecifically, without regard to the cell type.

For *in vivo* use, one would like to target therapeutic siRNA reagents to particular cell types (e.g., cancer cells), thereby limiting side effects that result from nonspecific delivery as well as reducing the quantity of siRNA necessary for treatment, an important cost consideration. One recent study described a promising approach in which antibodies that bind cell type–specific cell-surface receptors were fused to protamine and used to deliver siRNAs to cells via endocytosis[14]. Similarly, another study described a method to specifically deliver anti-ews-fli1 siRNAs to transferrin receptor–expressing tumors in mice using a cyclodextrin-containing polycation bearing transferrin as a targeting ligand[15].

Here, we describe a completely RNA-based approach for specific delivery of siRNAs. A number of groups have identified structured RNAs capable of binding a variety of proteins with high affinity and specificity with SELEX (systematic evolution of ligands by exponential enrichment). We decided to exploit the structural potential of RNA to target siRNAs to a cell-surface receptor specific to a particular cell type. Our approach relies on RNAs that include both a targeting moiety, the aptamer, and an RNA-silencing moiety, the siRNA, which is recognized and processed by Dicer in a manner similar to the processing of microRNAs (**Fig. 1a**).

We generated and tested aptamer-siRNA chimeric RNAs for their ability to (i) specifically bind prostate cancer cells expressing the cell-surface receptor PSMA using an RNA aptamer previously selected against human PSMA (A10)[16] and (ii) deliver therapeutic siRNAs that target polo-like kinase 1 (*PLK1*)[17] and *BCL2* (ref. 3), two survival genes overexpressed in most human tumors[18–20]. Because Dicer acts upon the chimeric RNAs, the siRNAs are directed into the RNAi pathway and silence their cognate mRNAs (**Fig. 1a**).

In contrast to most described delivery methods, this approach involves only RNA (that is, an RNA aptamer linked to an siRNA), an important advantage given the various side effects associated with many commonly used reagents such as proteins. Indeed, aptamer-siRNA chimeras present several advantages for *in vivo* applications. Aptamers and siRNAs have low immunogenicity. They can easily be synthesized in large quantities at a relatively low cost and are amenable to a variety of chemical modifications that confer both resistance to degradation and improved pharmacokinetics *in vivo*. The smaller size of aptamers compared with that of antibodies (<15 kDa versus

[1]Duke Center for Translational Research, Department of Surgery, [2]Duke Institute for Genome Sciences and Policy, Duke University Medical Center, Durham, North Carolina 27710, USA. [3]These authors contributed equally to this work. Correspondence should be addressed to B.A.S. (b.sullenger@cgct.duke.edu)

Received 3 March; accepted 23 May; published online 25 June 2006; doi:10.1038/nbt1223

150 kDa) facilitates their *in vivo* delivery by promoting better tissue penetration[21,22]. Importantly, the approach described here provides a means of cell type–specific siRNA delivery, which is a critical goal for the widespread therapeutic applicability of siRNAs.

RESULTS

A10 aptamer–siRNA chimeras

Aptamer–siRNA chimeric RNAs were generated to specifically target siRNAs to cells expressing the cell-surface receptor PSMA. The aptamer portion of the chimera (A10) mediates binding to PSMA. The siRNA portion targets the expression of the two survival genes *PLK1* (A10-Plk1) and *BCL2* (A10-Bcl2). A nonsilencing siRNA was used as a control (A10-CON). The RNA Structure Program (Version 4.1) was used to predict the secondary structures of A10 (data not shown) and the A10 aptamer–siRNA chimera derivatives (**Fig. 1b**). To predict the region of A10 responsible for binding to PSMA, we compared the predicted secondary structure of A10 to that of a truncated A10 aptamer, A10-3 (data not shown)[16]. Because A10-3 also binds PSMA, the structural component retained in A10-3 is likely to be necessary for binding PSMA (boxed in magenta in **Fig. 1b**). The predicted structures of the aptamer-siRNAs retain this predicted PSMA-binding component, suggesting that they should also retain PSMA binding (**Fig. 1b**, shown for A10-Plk1). As a control, we made two point mutations within this region (mutA10-Plk1) that are predicted to disrupt the secondary structure of the putative PSMA-binding portion of the A10 aptamer (**Fig. 1b**, shown in blue).

A10 chimeras bind PSMA-expressing cells

First, we tested the ability of the A10 aptamer–siRNA chimeras to bind the surface of cells expressing PSMA. Previously, PSMA has been shown to be expressed on the surface of LNCaP cells, but not on the surface of PC-3 cells (a distinct prostate cancer cell line), a finding we verified with flow cytometry and immunoblotting (**Supplementary Fig. 1** online). To determine whether the A10 aptamer–siRNA chimeras can bind the surface of cells expressing PSMA, we incubated fluorescently labeled A10, A10-CON (CON is a nontargeting siRNA) or A10-Plk1 with either LNCaP or PC-3 cells (**Fig. 1c**). Binding of A10 and A10 aptamer–siRNA chimeras was specific to LNCaP cells and was dependent on the region of A10 aptamer predicted to bind PSMA

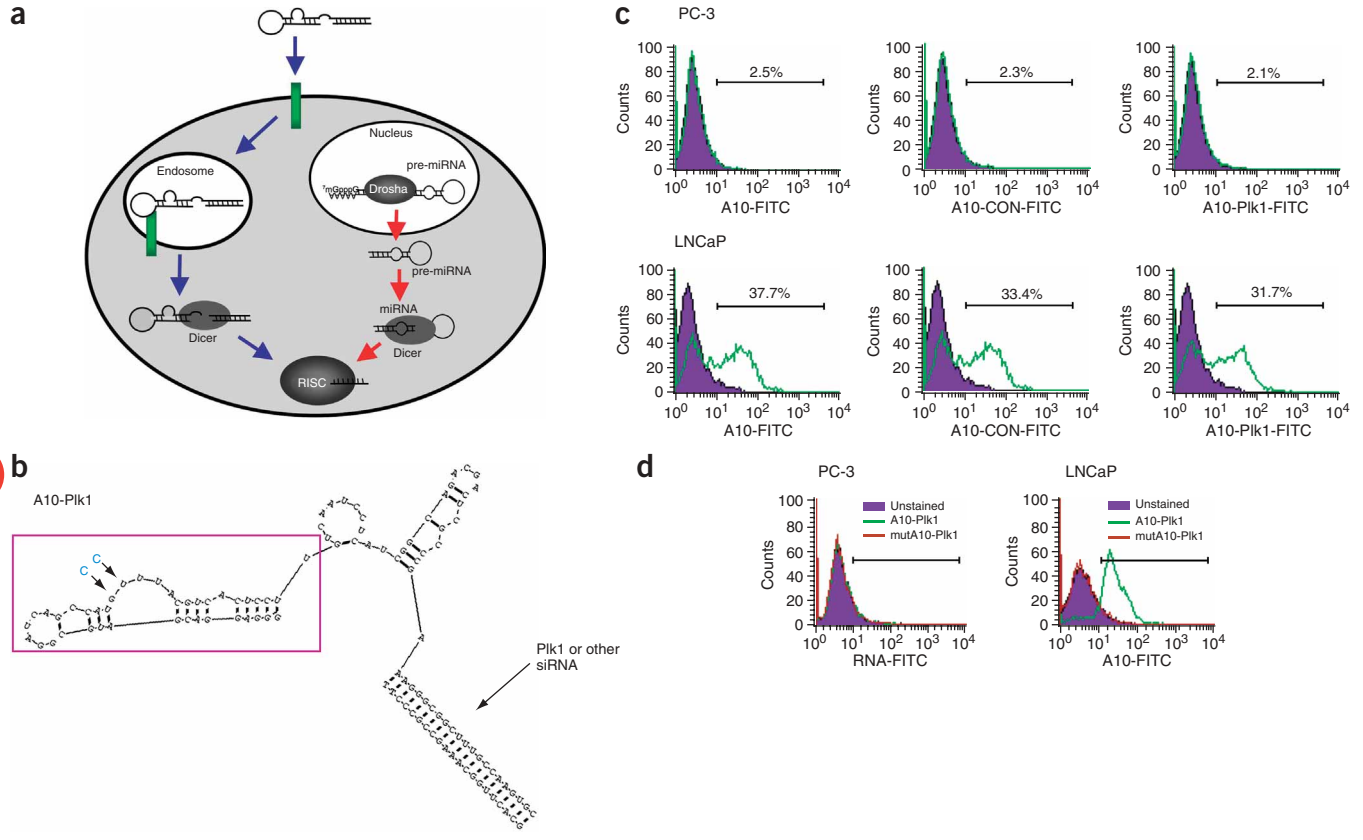

Figure 1 Proposed mechanism of action and predicted secondary structure of aptamer-siRNA chimeras. (**a**) The aptamer-siRNA chimera binds to the cell-surface receptor (light green rectangle), is endocytosed, and subsequently released from the endosome to enter the RNAi pathway. The endogenous microRNA silencing pathway is shown for comparison (red arrows). A pre-microRNA (pre-miRNA) exits the nucleus upon cleavage by Drosha, is recognized by the endonuclease Dicer, which processes the pre-miRNA into a 21nt mature miRNA. The mature miRNA is subsequently incorporated into the silencing complex (RISC) where it mediates targeted mRNA degradation. (**b**) Predicted secondary structure for the A10 aptamer–siRNA chimeras (A10-Plk1 depicted). The region of the A10 aptamer responsible for binding to PSMA is outlined in magenta. This region was mutated in the mutant A10 aptamer, mutA10-Plk1 (mutated bases shown in blue). Bold dashes in the structure represent base pairs, while finer dashes and lines represent covalent bonds. The siRNA portion of the chimera consists of 21 bps. (**c**) Cell-type specific binding of A10 aptamer–siRNA chimeras. FITC-labeled RNAs were tested for binding to PC-3 and LNCaP cells. Cell surface binding of FITC-labeled aptamer-siRNA chimeras (shown in green) was assessed by flow cytometry. Unstained cells are shown in purple. Binding was restricted to LNCaP cells expressing PSMA. (**d**) Binding of FITC-labeled A10-Plk1 (green) and mutA10-Plk1 (brown) to LNCaP and PC-3 cells as described for part **c**.

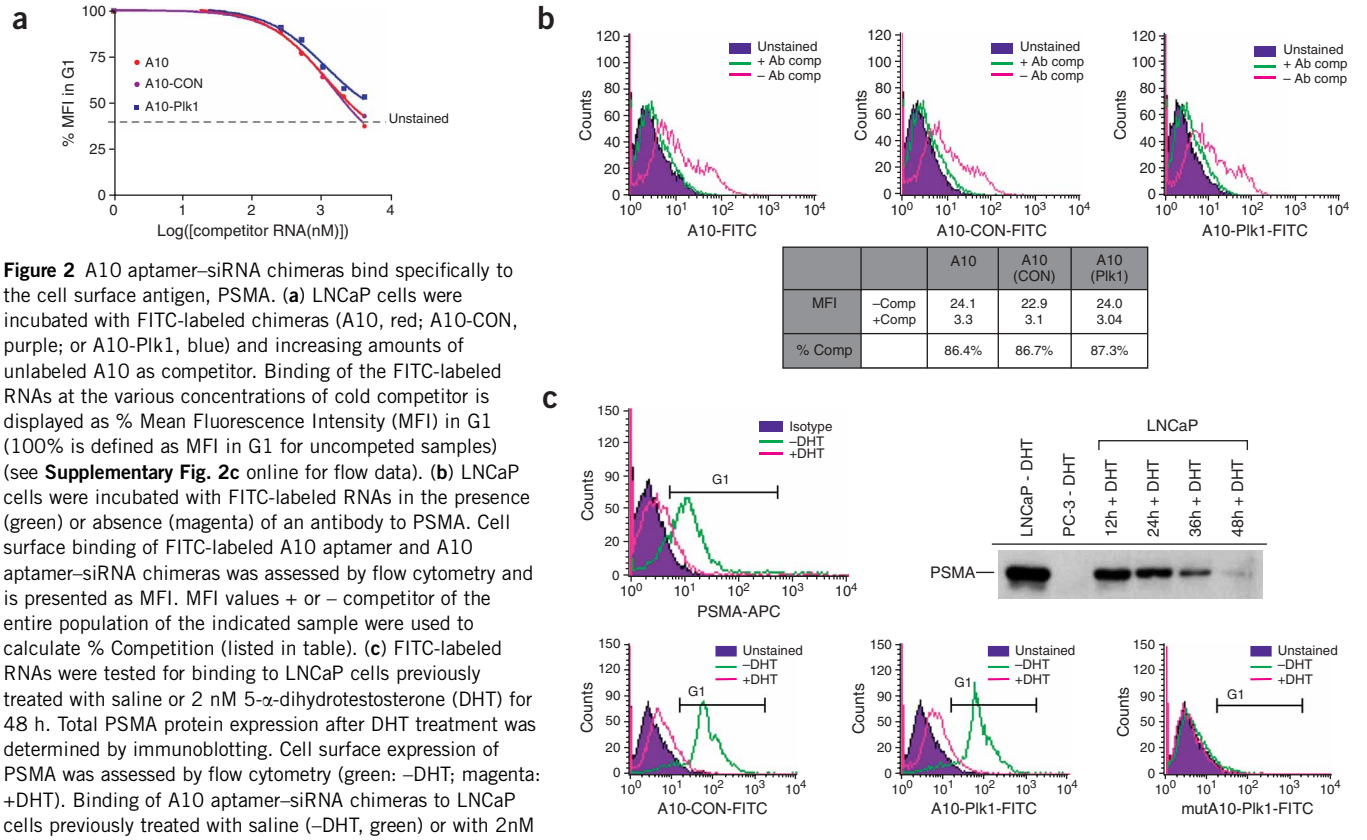

		A10	A10 (CON)	A10 (Plk1)
MFI	–Comp	24.1	22.9	24.0
	+Comp	3.3	3.1	3.04
% Comp		86.4%	86.7%	87.3%

Figure 2 A10 aptamer–siRNA chimeras bind specifically to the cell surface antigen, PSMA. (**a**) LNCaP cells were incubated with FITC-labeled chimeras (A10, red; A10-CON, purple; or A10-Plk1, blue) and increasing amounts of unlabeled A10 as competitor. Binding of the FITC-labeled RNAs at the various concentrations of cold competitor is displayed as % Mean Fluorescence Intensity (MFI) in G1 (100% is defined as MFI in G1 for uncompeted samples) (see **Supplementary Fig. 2c** online for flow data). (**b**) LNCaP cells were incubated with FITC-labeled RNAs in the presence (green) or absence (magenta) of an antibody to PSMA. Cell surface binding of FITC-labeled A10 aptamer and A10 aptamer–siRNA chimeras was assessed by flow cytometry and is presented as MFI. MFI values + or – competitor of the entire population of the indicated sample were used to calculate % Competition (listed in table). (**c**) FITC-labeled RNAs were tested for binding to LNCaP cells previously treated with saline or 2 nM 5-α-dihydrotestosterone (DHT) for 48 h. Total PSMA protein expression after DHT treatment was determined by immunoblotting. Cell surface expression of PSMA was assessed by flow cytometry (green: –DHT; magenta: +DHT). Binding of A10 aptamer–siRNA chimeras to LNCaP cells previously treated with saline (–DHT, green) or with 2nM DHT (magenta) was determined by flow cytometry.

as the mutA10-Plk1 was unable to bind (**Fig. 1d**). In addition, the aptamer-siRNA chimeras and the A10 aptamer were found to bind to the surface of LNCaP cells with comparable affinities (**Supplementary Fig. 2** online).

To verify that the A10 aptamer–siRNA chimeras were indeed binding to PSMA, we incubated LNCaP cells with fluorescently labeled A10, A10-CON, or A10-Plk1 RNA (1 μM) and used increasing amounts (from 0 μM to 4 μM) of unlabeled A10 aptamer (**Fig. 2a**) or an antibody specific for human PSMA as competitors against the labeled chimeras (**Fig. 2b**). We assessed the binding of fluorescently labeled RNAs in the presence of increasing amounts of competitor using flow cytometry (**Fig. 2a**; also see **Supplementary Fig. 2c** online for primary data). Binding of the labeled A10 aptamer and A10 aptamer–siRNA chimeras (A10-CON and A10-Plk1) to LNCaP cells competed equally well with binding of either unlabeled A10 or the anti-PSMA antibody, indicating that the aptamer-containing RNAs are binding PSMA on the surface of LNCaP cells. To further confirm that the target of the aptamer-siRNA chimeras is indeed PSMA, we tested binding of the chimeras on LNCaP cells pretreated with 5-α-dihydrotestosterone (DHT), as DHT has been shown to reduce the expression of PSMA[23]. We measured DHT-mediated inhibition of PSMA gene expression by immunoblotting. Cell surface reduction of PSMA protein (from 73.2% to 13.4%) was verified by flow cytometry (**Fig. 2c**, top panel). Reduced cell surface expression of PSMA correlated with reduced binding of A10-CON (from 89.7% to 6.7%) and A10-Plk1 (from 90.7% to 9.7%) to LNCaP cells (**Fig. 2c**). As expected, mutA10-Plk1 did not bind to the surface of LNCaP cells either in the presence or absence of DHT treatment (**Fig. 2c**).

A10 chimeras specifically silence gene expression

To determine whether the aptamer-siRNA chimeras can silence target gene expression, we used A10 aptamer–siRNA chimeras to deliver siRNAs against *PLK1* (ref. 17) or *BCL2* (ref. 3) to cells expressing PSMA (**Fig. 3**). PC-3 and LNCaP cells were treated with aptamer-siRNA chimeras A10-Plk1 (**Fig. 3a**) or A10-Bcl2 (**Fig. 3c**) in the absence of transfection reagents. Silencing of *PLK1* and *BCL2* was assessed by flow cytometry (**Fig. 3a,c**) and quantitative RT-PCR (qRT-PCR) (**Fig. 3b,d**). As a control for qRT-PCR, cells were transfected with nonsilencing siRNAs (con siRNA) or siRNAs to *PLK1* or *BCL2* (*PLK1* siRNA or *BCL2* siRNA). In contrast to transfection of the nontargeted siRNAs (**Supplementary Fig. 3** online), silencing by A10-Plk1 and A10-Bcl2 was specific to LNCaP cells expressing PSMA and correlated with binding/uptake of fluorescent-labeled aptamer-siRNA chimeras in LNCaP cells (**Fig. 3a,c**). The cell type–specific reduction in Plk1 and Bcl2 proteins indicates that the siRNAs are being delivered specifically to PSMA-expressing cells via the aptamer portion of the chimeras. To further verify that silencing by A10 aptamer–siRNA chimeras was indeed dependent on PSMA, we incubated LNCaP cells with or without 2 nM DHT for 48 h before addition of A10-Plk1 (**Fig. 3e**). Binding/uptake of A10-Plk1 in cells and silencing of *PLK1* expression were substantially decreased in cells treated with DHT. These data, together with the cell surface binding data, indicate that cell type–specific silencing is dependent upon cell surface expression of PSMA.

Functional characterization of A10 chimeras

To determine whether the aptamer-siRNA chimeras targeting oncogenes and anti-apoptotic genes reduce cell proliferation and induce apoptosis, we measured these cellular processes in cells treated with

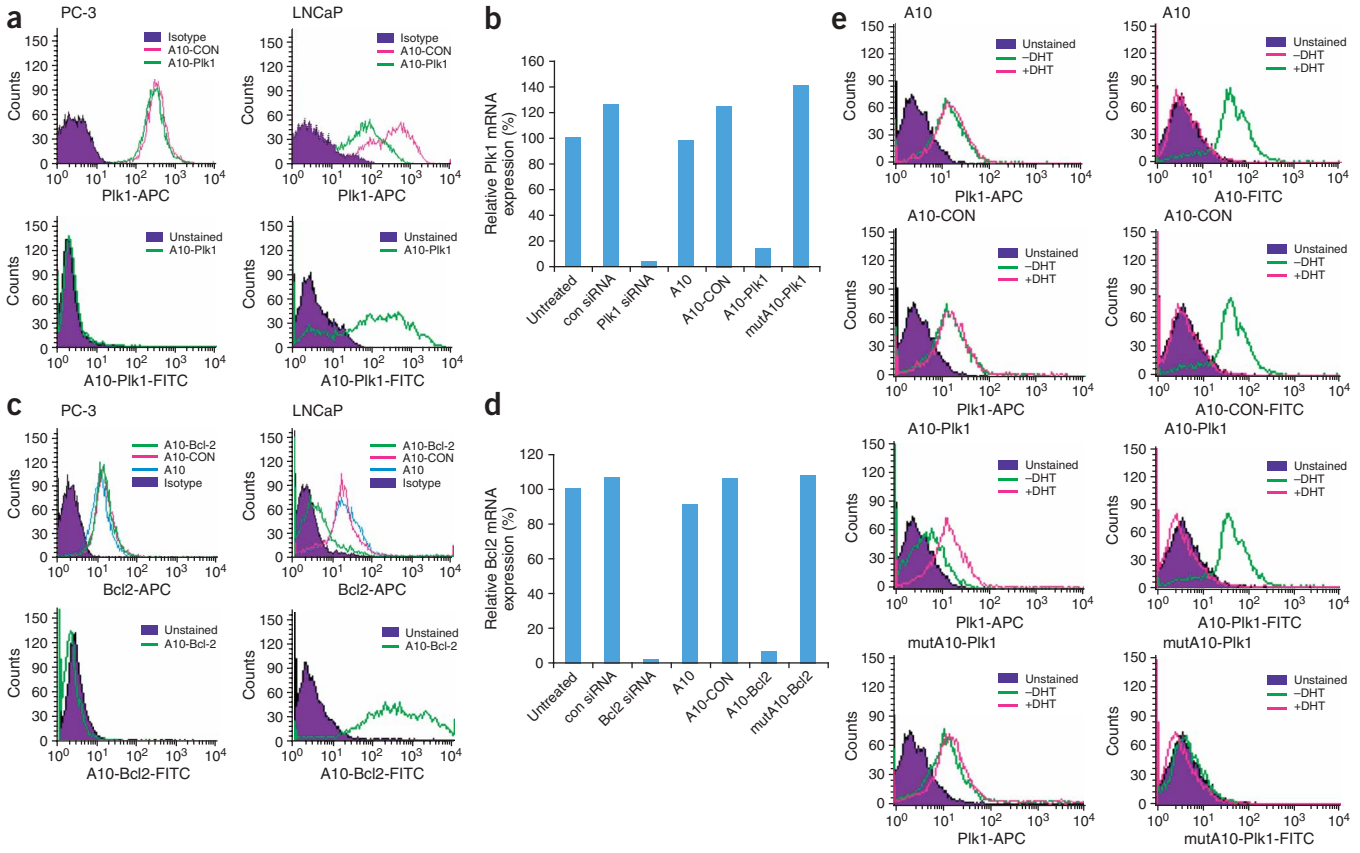

Figure 3 Cell-type specific silencing of genes with aptamer-siRNA chimeras. LNCaP and PC-3 cells were incubated with the various FITC-labeled aptamer-siRNA chimeras for 48 h in the absence of transfection reagents. (**a–d**) Silencing of either *PLK1* (**a**,**b**) or *BCL2* (**c**,**d**) expression was assessed by flow cytometry (**a**,**c**) using antibodies specific to human Plk1 and human Bcl2, respectively (top panels) or by quantitative RT-PCR (**b**,**d**). Gene silencing was restricted to LNCaP cells and correlated with efficient labeling in LNCaP cells with FITC-labeled RNAs (green) as determined by flow cytometry (bottom panels). Unstained cells or isotype control are shown in purple; A10 (blue), A10-CON (magenta), A10-Plk1 and A10-Bcl2 (green). (**e**) A10-Plk1 mediated silencing of Plk1 in LNCaP cells previously treated with saline (–DHT, green) or with 2 nM DHT (magenta) for 48 h (left panels), and corresponding FITC-labeled RNA cell labeling (right panels).

the chimeras. PC-3 and LNCaP cells were treated with A10-CON or A10-Plk1 aptamer-siRNA chimeras (**Fig. 4a**) and cell proliferation was measured by ^{3}H-thymidine incorporation. In LNCaP cells, proliferation was effectively reduced by the A10-Plk1 chimera but not by the control A10-CON chimera. This effect was specific for cells expressing PSMA as it was not seen in the PC-3 cells. Proliferation was reduced to nearly the same extent as observed when cationic lipids were used to transfect *PLK1* siRNA, even though no transfection reagent was used for aptamer-siRNA chimera delivery (**Fig. 4a**).

Next, we assessed the ability of the A10-Plk1 and A10-Bcl2 chimeras to induce apoptosis of prostate cancer cells expressing PSMA (**Fig. 4b**,**c**). PC-3 and LNCaP cells were either treated by addition of A10, A10-CON, A10-Plk1 or A10-Bcl2, to the media or transfected with siRNAs to *PLK1* or *BCL2* using cationic lipids. Apoptosis was assessed by measuring production of active caspase 3 (Casp3) by flow cytometry. Whereas transfected *PLK1* and *BCL2* siRNAs induced apoptosis of both PC-3 and LNCaP cells, the aptamer-siRNA chimeras induced apoptosis only of LNCaP cells and did not require a transfection reagent. Treatment of PC-3 and LNCaP cells with cisplatin was used as a positive control for apoptosis (**Fig. 4b**).

Mechanism of chimera-mediated gene silencing

We sought to determine whether the mechanism by which aptamer-siRNA chimeras silence gene expression is dependent on Dicer activity. Therefore, the Dicer protein level was reduced by targeting its expression with an siRNA against human Dicer[24] (**Supplementary Fig. 4** online). Next, A10-Plk1 chimera–mediated gene silencing was tested for its dependence on Dicer expression. LNCaP cells were cotransfected with aptamer-siRNA chimeras (A10-CON or A10-Plk1) alone or together with the Dicer siRNA (**Fig. 5a**). Silencing of *PLK1* expression by the A10-Plk1 chimera was inhibited by cotransfection of Dicer siRNA (**Fig. 5a**, top panels), suggesting that aptamer-siRNA chimera–mediated gene silencing is dependent on Dicer and occurs via the RNAi pathway. In contrast, inhibition of Dicer had no effect on transfected *PLK1* siRNA-mediated silencing (**Fig. 5a**, bottom panels), as 21- to 23-nt long siRNAs have been shown to bypass the Dicer step[25,26].

To test whether the aptamer-siRNA chimeras were directly cleaved by Dicer to produce 21- to 23-nt siRNA fragments corresponding to the siRNA sequences engineered in the chimeric constructs, we incubated the RNAs with recombinant Dicer enzyme *in vitro* and the resulting fragments were resolved with nondenaturing PAGE (**Fig. 5b**,**c**). The aptamer-siRNA chimeras (A10-CON or A10-Plk1), but not A10 or the longer single-stranded sense strand of the aptamer-siRNA chimeras (ssA10-CON or ssA10-Plk1), were digested by the Dicer enzyme to release 21- to 23-nt fragments in length (**Fig. 5b**). To verify that these 21- to 23-nt long Dicer fragments corresponded to the control and *PLK1* siRNAs, we labeled the A10-aptamer-siRNA

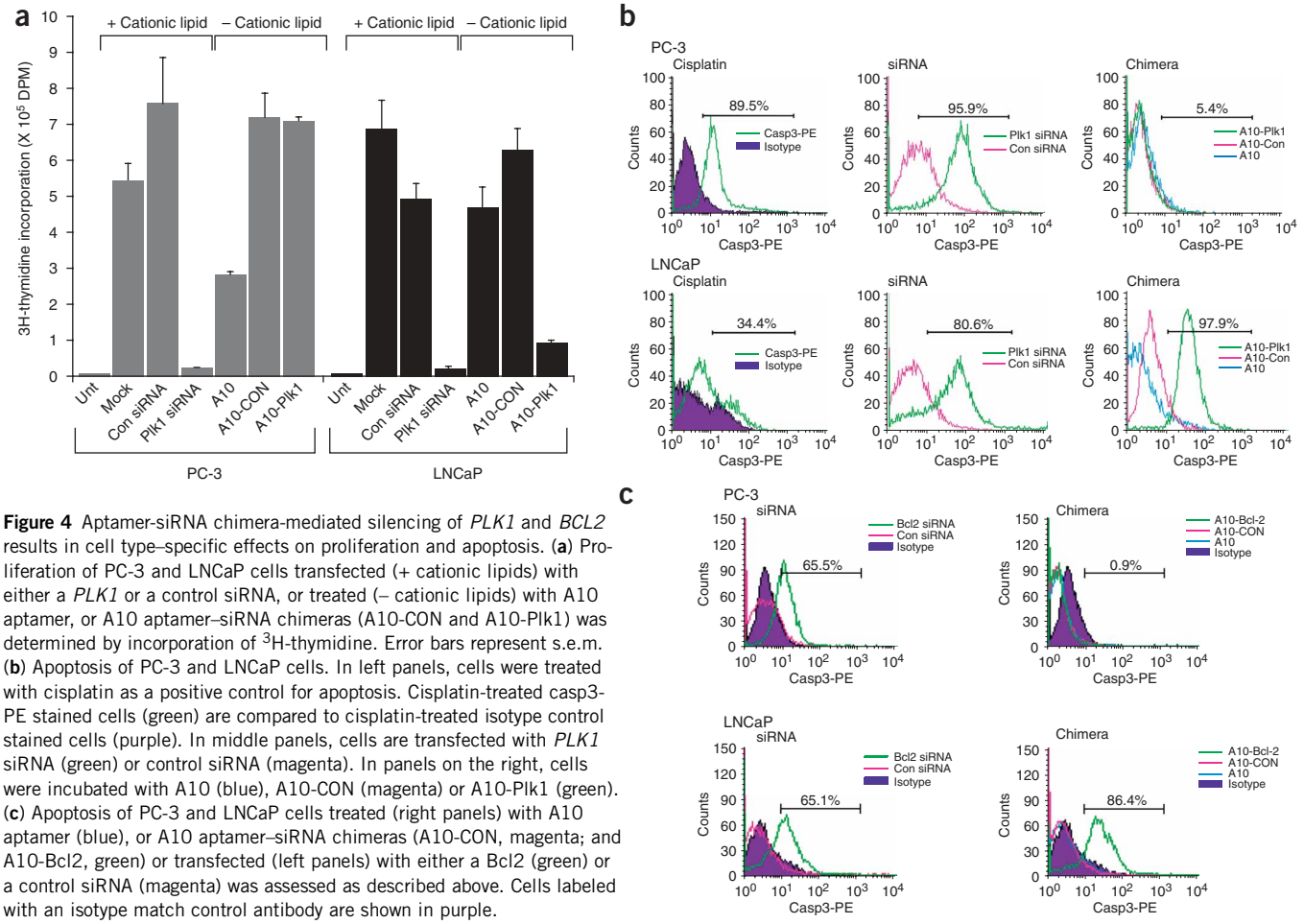

Figure 4 Aptamer-siRNA chimera-mediated silencing of *PLK1* and *BCL2* results in cell type–specific effects on proliferation and apoptosis. (**a**) Proliferation of PC-3 and LNCaP cells transfected (+ cationic lipids) with either a *PLK1* or a control siRNA, or treated (– cationic lipids) with A10 aptamer, or A10 aptamer–siRNA chimeras (A10-CON and A10-Plk1) was determined by incorporation of ^{3}H-thymidine. Error bars represent s.e.m. (**b**) Apoptosis of PC-3 and LNCaP cells. In left panels, cells were treated with cisplatin as a positive control for apoptosis. Cisplatin-treated casp3-PE stained cells (green) are compared to cisplatin-treated isotype control stained cells (purple). In middle panels, cells are transfected with *PLK1* siRNA (green) or control siRNA (magenta). In panels on the right, cells were incubated with A10 (blue), A10-CON (magenta) or A10-Plk1 (green). (**c**) Apoptosis of PC-3 and LNCaP cells treated (right panels) with A10 aptamer (blue), or A10 aptamer–siRNA chimeras (A10-CON, magenta; and A10-Bcl2, green) or transfected (left panels) with either a Bcl2 (green) or a control siRNA (magenta) was assessed as described above. Cells labeled with an isotype match control antibody are shown in purple.

chimeras by annealing the complementary ^{32}P-end labeled anti-sense strand of the siRNAs and incubated with or without recombinant Dicer (**Fig. 5c**). Digestion of labeled A10-CON or A10-Plk1 with recombinant Dicer resulted in release of 21- to 23-nt long fragments that retained the ^{32}P-end labeled anti-sense strand, indicating that these fragments are indeed the siRNA portion of the aptamer-siRNA chimeras.

To further verify that the RNA chimera-mediated gene silencing was due to siRNA-directed cleavage, we characterized specific cleavage products of *PLK1* mRNA using a modified 5′-RACE (rapid amplification of cDNA ends) approach as previously described[10]. mRNA from LNCaP cells transfected with either control siRNA (CON), *PLK1* siRNA, A10-CON or A10-Plk1 was isolated and 5′-RACE and PCR were used to reveal fragments of the predicted length in cells treated with *PLK1* siRNA or A10-Plk1 (**Fig. 5d**). The identity of the expected PCR product was verified by direct sequencing of the amplified products, which demonstrated that cleavage occurred at the predicted position for the siRNA duplex, ten nucleotides downstream of the 5′ end of the *PLK1* siRNA antisense strand. No fragments were detected in control cells (untreated, con siRNA, or A10-CON).

A10 chimeras do not trigger interferon responses

Various groups have reported that delivered siRNAs can potentially activate nonspecific inflammatory responses, leading to cellular toxicity[27,28]. Therefore, we determined the amount of INF-β produced by PC-3 and LNCaP cells that were either untreated, transfected with siRNAs to *PLK1* or *BCL2*, or treated with the aptamer-siRNA chimeras using an enzyme-linked immunosorbent assay (ELISA) (**Supplementary Fig. 5** online). Treatment with either siRNAs or aptamer-siRNA chimeras did not induce production of INF-β under these experimental conditions, suggesting that delivery of aptamer-siRNA chimeras does not trigger a substantial type I interferon response in these cells.

A10-Plk1 promotes tumor regression

We next assessed the efficiency and specificity of the A10-Plk1 chimera for its ability to limit tumor growth in athymic mice bearing tumors derived from either PSMA-positive human prostate cancer cells (LNCaP) or PSMA-negative human prostate cancer cells (PC-3) (**Fig. 6**; see **Supplementary Fig. 6** online for individual tumor curves). Athymic mice were inoculated with either LNCaP or PC-3 cells and tumors were allowed to grow until they reached 1 cm in diameter in the longest dimension. Tumors were then injected (Day 0) with either 100 µl DPBS alone or with 100 µl (200 pmoles) chimeric RNAs (A10-CON, A10-Plk1 or mutA10-Plk1) every other day for a total of ten injections administered. The variability of infusate distribution was determined and is described in **Supplementary Figure 6b** online. Tumors were measured every 3 d. No difference in tumor volume was observed with the PC-3 tumors with any of the different treatments indicating that the chimeric RNAs did not have any nonspecific cell killing effect. In contrast, a pronounced reduction in tumor volume

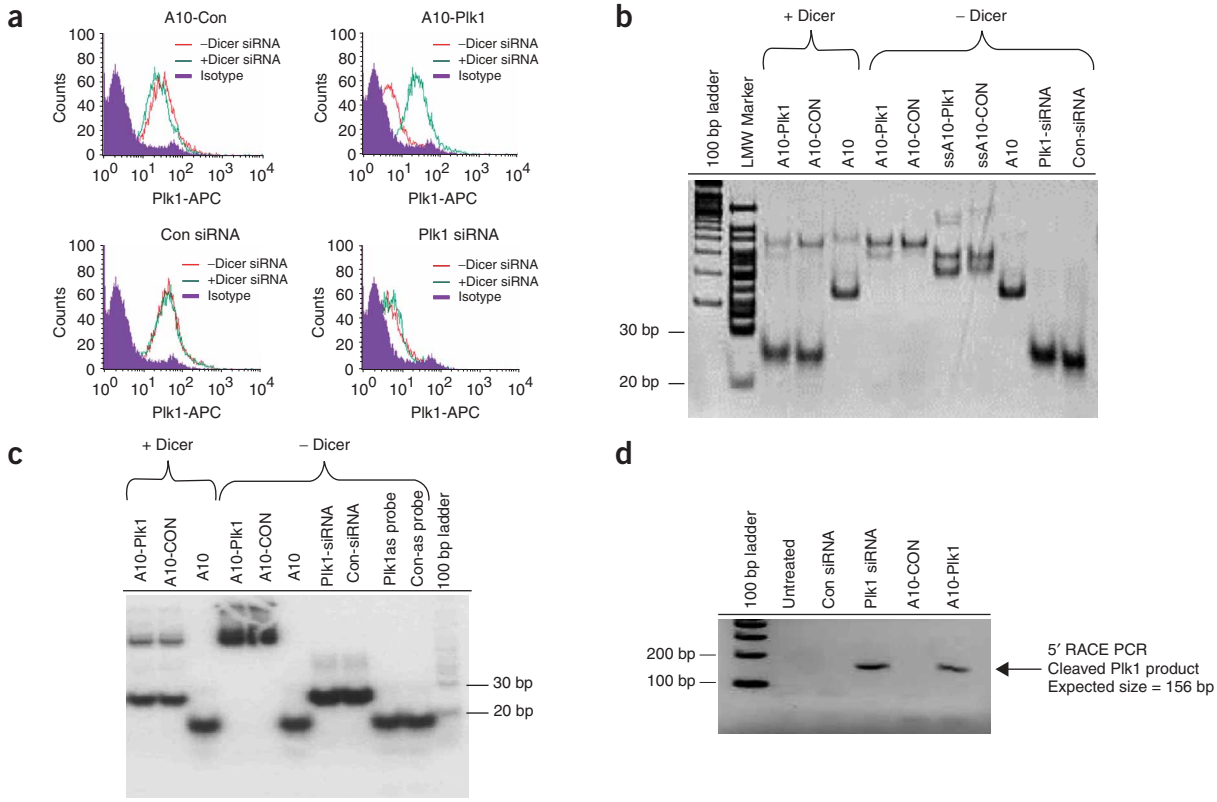

Figure 5 Aptamer-siRNA chimera-mediated gene silencing occurs via the RNAi pathway. (**a**) LNCaP cells were transfected with either siRNAs or A10 aptamer–siRNA chimeras (A10-CON and A10-Plk1) in the presence (green) or absence (red) of siRNA against Dicer. Cells were then analyzed for *PLK1* gene expression by flow cytometry as described above. Isotype controls are shown in purple. (**b**) *In vitro* Dicer assay. The indicated RNAs treated with or without recombinant Dicer were resolved on a nondenaturing polyacrylamide gel and stained with ethidium bromide. ssA10-Plk1 and ssA10-CON are single-stranded chimeras without antisense siRNA. (**c**) *In vitro* Dicer assay. Aptamer-siRNA chimeras annealed to the complementary antisense siRNA strand labeled with ^{32}P, were incubated with or without Dicer and cleavage products were subsequently resolved on a nondenaturing polyacrylamide gel. The antisense siRNAs were not complementary to and thus did not anneal to A10 (lanes 3 and 6). (**d**) Cleaved mRNA from LNCaP cells previously transfected with either saline (untreated), con siRNA, Plk1 siRNA, A10-CON, or A10-Plk1 RNAs, was ligated to an RNA adaptor and reverse transcribed using a gene-specific primer. Agarose gel of 5′RACE-PCR amplification, using a primer specific to the RNA adaptor and a reverse primer to *PLK1*, showing specific siRNA-mediated cleavage products of *PLK1* mRNA.

was observed for LNCaP tumors treated with the A10-Plk1 chimera. Indeed, from day 6 to day 21 the various control-treated tumors increased 3.63-fold in volume ($n = 22$), whereas the A10-Plk1-treated tumors had a 2.21-fold reduction in volume ($n = 8$) ($P<0.0001$) (**Fig. 6a**). Regression of LNCaP tumor volume was specific to the A10-Plk1 group and was not observed with DPBS treatment or treatment with the A10-CON or mutA10-Plk1 chimeric RNAs. Notably, no morbidity or mortality was observed following the 20-d treatment with the chimeric RNAs, suggesting that these compounds are not toxic to the animals under the conditions of these experiments. Histological examination of the tumor sections revealed that in contrast to PBS or A10-CON-treated tumors, tumors treated with A10-Plk1 were vacuolated (evidence of cell ghosts), had extensive granulation and had evidence of necrosis. Moreover, less epithelium was present in the area of the tumor. Conversely, the control tumors were dense and composed primarily of epithelium. Occasional pockets of necrosis were observed in the mutA10-Plk1-treated tumors, suggesting that nonspecific uptake and subsequent processing of this chimera may have occurred to a limited extent in these tumors. However, no substantial change in tumor volume was noted in the mutA10-Plk1 treated tumors, indicating that this uptake was a very inefficient process.

DISCUSSION

We have developed and characterized aptamer-siRNA chimeras that target specific cell types and act as substrates for Dicer, thereby triggering cell type–specific gene silencing. In this proof-of-concept study, we have targeted anti-apoptotic genes with RNAi specifically in cancer cells expressing the cell-surface receptor PSMA. Depletion of the targeted gene products resulted in decreased proliferation and increased apoptosis of the targeted cells in culture (**Fig. 4**). Cellular targeting of the chimeric RNAs was mediated by the interaction of the aptamer portion of the chimeras with PSMA on the cell surface. Notably, a mutant chimeric RNA bearing two point mutations within the region of the aptamer responsible for binding to PSMA resulted in loss of binding activity (**Fig. 1d**). Binding specificity was further verified by demonstrating that PC-3 cells, which do not express PSMA, and LNCaP cells depleted of PSMA by treatment with 5-α-dihydrotestosterone were not targeted by the chimeras, whereas untreated LNCaP cells, which express PSMA, were targeted (**Fig. 2c**). Additionally, antibodies specific for PSMA competed for binding of the chimeras to the LNCaP cell surface (**Fig. 2b**).

We have shown that gene silencing by the chimeric RNAs is dependent on the RNAi pathway because it requires Dicer, an endonuclease that processes dsRNAs before assembly of RNA-induced

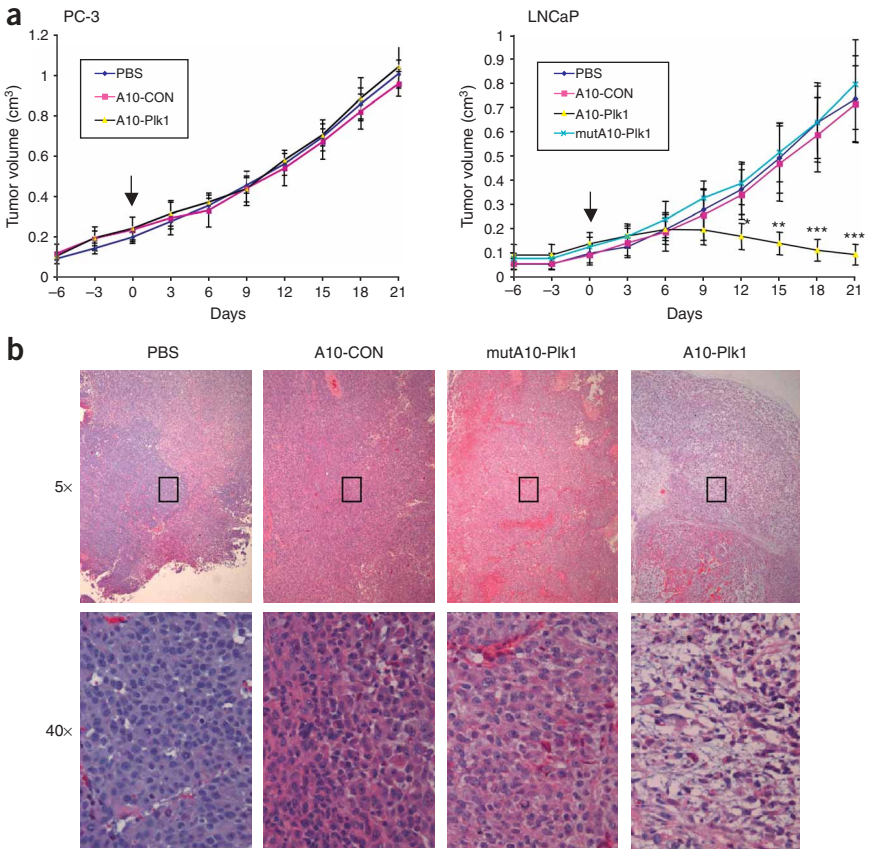

Figure 6 Antitumor activity of A10-Plk1 aptamer-siRNA chimera in a xenograft model of prostate cancer. (**a**) Chimeric RNAs (A10-CON, magenta; A10-Plk1, yellow; mutA10-Plk, light blue) were administered intratumorally in a mouse xenograft model bearing either PSMA-negative prostate cancer cells, PC-3 (left panel) or PSMA-positive prostate cancer cells, LNCaP (right panel) implanted bilaterally into the hind flanks of nude mice. Saline (PBS) treated animals were used as a control (dark blue). Tumors were measured every three days. The mean tumor volumes were analyzed using a one-way ANOVA. ***, $P<0.0001$; **, $P<0.001$; *, $P<0.01$ ($n = 6$–8 tumors). (**b**) Histology of LNCaP tumors treated with the various chimeras. Serial sections of formalin-fixed tumors embedded in paraffin were stained with hematoxylin and eosin (H&E) and analyzed at 5× and 40× magnification (boxed region is amplified eight times in the bottom panels). Note reduction in cell density in the A10-Plk1 treated section.

silencing complexes (RISC) (**Fig. 5a**). Dicer was also found to cleave the double-stranded, gene-targeting portion of the chimeras from the aptamer portion, a step that would be expected to precede incorporation of the shorter strand of these reagents into RISC (**Fig. 5b**,**c**). Finally, we showed that the chimeric-siRNA mediates *PLK1* mRNA cleavage at the predicted position for the siRNA, ten nucleotides downstream of the 5′ end of the *PLK1* siRNA antisense strand (**Fig. 5d**).

Notably, this siRNA delivery approach effectively mediated tumor regression in a xenograft model of prostate cancer (**Fig. 6**). The RNA chimeras are therefore suitable for targeting tumors in mice *in vivo* in the form in which we have generated them and may, in the future, prove to be useful therapeutics for treating human prostate cancer. These reagents exhibited the same specificity for PSMA expression *in vivo* as they did *in vitro*, as the PSMA-negative PC-3 tumors did not regress when treated. It is noteworthy that the RNA used to make the chimeras is protected from rapid nuclease degradation by the 2′-fluoro modification of the pyrimidines in the aptamer sense strand, which is likely to be essential for their performance *in vivo* (as well as *in vitro* in the presence of serum)[29–31].

Whereas various methods have been described for delivering siRNAs to cells, most of these methods accomplish delivery nonspecifically[3–13]. Cell type–specific delivery of siRNAs is therefore a critical goal for the widespread applicability of this technology in therapeutics because of both safety and cost considerations. Delivery of siRNAs to nontargeted cells can result in various adverse side effects. For example, siRNAs are known to activate toll-like receptors within plasmacytoid dendritic cells, leading to interferon secretion, which can result in various adverse symptoms[27,28]. In the case of delivering siRNAs that trigger apoptosis, another danger is that nonspecific delivery will kill healthy cells, which could certainly cause problems in a clinical setting. Treatments involving systemic delivery of siRNAs would be expected to require substantially less of a targeted (as compared with a nontargeted) reagent because of the reduction in uptake by nontargeted cells. Thus, targeting approaches for therapeutic use of siRNA may substantially reduce the cost of the therapy.

The siRNA-aptamer chimeras also may have important advantages over other methods for targeted delivery of siRNAs in terms of cost and production, flexibility regarding chemical modification and safety. Notably, the approach developed here is compatible with chemical synthesis of RNAs. Short RNA aptamers (25–35 bases) that bind various targets with high affinities have been described[21,22]. Chimeras designed with such short aptamers would have a long strand of ~45–55 bases, a length that can currently be produced with chemical synthesis. (It may be possible to further truncate the A10 aptamer to produce a chimeric oligo that can be even more economically synthesized.) In contrast, protein reagent production in cell culture is considerably more complex and difficult to control. Moreover, chemically synthesized RNA is amenable to various modifications such as pegylation that can be used to modify its *in vivo* half-life and bioavailability. Of course, in the case of the siRNA-aptamer chimeras, such modifications would need to be tested to determine whether they interfere with mechanisms such as uptake and processing by Dicer. An additional, notable advantage of the chimera over alternative approaches is its simplicity. Like siRNAs, the chimera consists only of RNA, and any nonspecific side effects may therefore be limited to those already produced by the siRNAs themselves. As RNA is believed to be less immunogenic than protein, the chimeric RNAs would also be expected to produce less nonspecific activation of the immune system than protein-mediated delivery approaches. This fact of RNA may be an important difference as a number of proteins currently used for therapeutics are known to occasionally cause dangerous allergic reactions, especially following repeated administration[32,33].

For many potential therapeutic applications of chimeras, such as targeting tumor vasculature and metastases, it will likely be necessary to administer the chimeras systemically. For such applications, the

pharmacokinetics and biodistribution of chimeras need to be measured to determine the best possible formulation, delivery approach and dose for each particular application. As mentioned above, pegylation is a fairly well-characterized modification that may extend the systemic half-life of chimeras, which is a potential problem because short nucleotides are rapidly cleared by the kidneys. Multimerizing the chimeras by increasing their size might make renal clearance less likely. Although it is difficult to determine from our data what dose might be effective in a systemic administration, another likely result of multimerizing the chimeras is to increase their avidity for the cell surface, thereby potentially reducing the necessary dose.

It has been proposed that Dicer-mediated processing of RNAs may result in more efficient incorporation of resulting siRNAs into RISC[26]. This suggestion is based on the observation that longer double-stranded RNAs (~29 bps), which are processed by Dicer, deplete their cognate mRNAs at lower concentrations than 19- to 21-bp siRNAs, which are not processed by Dicer. Thus, it is tempting to speculate that because the chimeras are processed by Dicer they may be more potent in terms of gene-silencing ability than dsRNAs of 19–21 bps that are not processed.

Because PSMA, the cell-surface target of the chimeras, is expressed in prostate cancer cells and the vascular endothelium of most solid tumors, the particular reagents we have developed may in the future have applications in treating prostate and other cancers. However, the approach developed here can, in principle, be adapted to generate therapeutics to treat a wide variety of diseases in addition to cancer. The two requirements for developing this approach for a given disease are that silencing specific genes in a defined population of cells will produce therapeutic benefits and that there are surface receptors expressed specifically on the cell population of interest that can deliver RNA ligands intracellularly. We think that many diseases are likely to satisfy both of these requirements and may in the future be treatable with the approach demonstrated here.

METHODS

Materials. Unless otherwise noted, all chemicals were purchased from Sigma-Aldrich, all restriction enzymes were obtained from New England BioLabs (NEB) and all cell culture products were purchased from Gibco BRL/Life Technologies, a division of Invitrogen.

siRNAs. con siRNA target sequence: 5′-AATTCTCCGAACGTGTCACGT-3′
PLK1 siRNA target sequence: 5′-AAGGGCGGCTTTGCCAAGTGC-3′
BCL2 siRNA target sequence: 5′-NNGTGAAGTCAACATGCCTGC-3′
Dicer siRNA target sequence: 5′-NNCCTCACCAATGGGTCCTTT-3′
Fluorescent siRNAs labeled with FITC at the 5′ end of the antisense strand were purchased from Dharmacon.

Aptamer-siRNA chimeras. A10: 5′-GGGAGGACGAUGCGGAUCAGCCAUGUUUACGUCACUCCUUGUCAAUCCUCAUCGGCAGACGACUCGCCCGA-3′
A10-CON sense strand: 5′-GGGAGGACGAUGCGGAUCAGCCAUGUUUACGUCACUCCUUGUCAAUCCUCAUCGGCAGACGACUCGCCCGA**AAUUCUCCGAACGUGUCACGU**-3′
A10-CON Antisense siRNA: 5′-ACGUGACACGUUCGGAGAAdTdT-3′
A10-Plk1 sense strand: 5′-GGGAGGACGAUGCGGAUCAGCCAUGUUUACGUCACUCCUUGUCAAUCCUCAUCGGCAGACGACUCGCCCGA**AAGGGCGGCUUUGCCAAGUGC**-3′
A10-Plk1 Antisense siRNA: 5′-GCACUUGGCAAAGCCGCCCdTdT-3′
A10-Bcl2 sense strand: 5′-GGGAGGACGAUGCGGAUCAGCCAUGUUUACGUCACUCCUUGUCAAUCCUCAUCGGCAGACGACUCGCCCGA**AAGUGAAGUCAACAUGCCUGC**-3′
A10-Bcl2 Antisense siRNA: 5′-GCAGGCAUGUUGACUUCACUU-3′
mutA10-Plk1 sense strand: 5′-GGGAGGACGAUGCGGAUCAGCCAU***CC***UUACGUCACUCCUUGUCAAUCCUCAUCGGCAGACGACUCGCCCGA**AAGGGCGGCUUUGCCAAGUGC**-3′
A10-Plk1 Antisense siRNA: 5′-GCACUUGGCAAAGCCGCCCdTdT-3′
A10 5′-primer: 5′-TAATACGACTCACTATAGGGAGGACGATGCGG-3′
A10 3′-primer: 5′-TCGGGCGAGTCGTCTG-3′
A10 template primer: 5′-GGGAGGACGATGCGGATCAGCCATGTTTACGTCACTCCTTGTCAATCCTCATCGGCAGACGACTCGCCCGA-3′
Control siRNA 3′-primer: 5′-**ACGTGACACGTTCGGAGAATT**TCGGGCGAGTCGTCTG-3′
Plk1 siRNA 3′-primer: 5′-**GCACTTGGCAAAGCCGCCCTT**TCGGGCGAGTCGTCTG-3′
Bcl2 siRNA 3′-primer: 5′**GCAGGCATGTTGACTTCACTT**TCGGGCGAGTCGTCTG-3′
A10 mutant primer: 5′-AGGACGATGCGGATCAGCCATCCTTACGTCA-3′

Double-stranded DNA templates were generated by PCR as follows. The A10 template primer was used as a template for the PCRs with the A10 5′-primer and one of the following 3′-primers: A10 3′-primer (for the A10 aptamer), control siRNA 3′-primer (for the A10-CON chimera), *PLK1* siRNA 3′-primer (for the A10-Plk1 chimera) or *BCL2* siRNA 3′-primer (for the A10-Bcl2 chimera). Templates for transcription were generated in this way or by cloning these PCR products into a T-A cloning vector (pGem-t-easy, Promega) and using the clones as templates for PCR with the appropriate primers.

The DNA encoding the mutA10-Plk1 chimera was prepared by sequential PCRs. In the first reaction, the A10 template primer was used as the template with the A10 mutant primer as the 5′-primer and the *PLK1* siRNA 3′-primer as the 3′-primer. The product of this reaction was purified and used as the template for a second reaction with the A10 5′-primer and the *PLK1* siRNA 3′-primer. The resulting PCR product was cloned into pGem-t-easy and sequenced. This clone was used as the template in a PCR with the A10 5′-primer and the Plk-1 3′-primer to generate the template for transcription. Fluorescent aptamer and aptamer-siRNA chimeras were *in vitro* transcribed in the presence of 5′-(FAM)(spacer 9)-G-3′ (FAM-labeled G) (TriLink) as described below. To prepare chimeras, 10 μM gel-purified sense RNA was combined with 20 μM of the appropriate antisense RNA in DPBS, heated to 65 °C for 5 min and then incubated at 37 °C for 10 min.

***In vitro* transcriptions.** Transcriptions were set up either with or without 4 mM FAM-labeled G. For a 250 μl transcription reactions: 50 μl 5× T7 RNAP buffer optimized for 2′F transcriptions (20% wt/vol PEG 8000, 200 mM Tris-HCl pH 8.0, 60 mM $MgCl_2$, 5mM spermidine HCl, 0.01% wt/vol Triton X-100, 25 mM DTT), 25 μl 10× 2′F-dNTPs (30 mM 2′F-CTP, 30 mM 2′F-UTP, 10 mM 2′OH-ATP, 10 mM 2′OH-GTP), 2 μl IPPI (Roche), 300 pmoles aptamer-siRNA chimera PCR template, 3 μl T7(Y639F) polymerase[34], bring up to 250 μl with milliQ H_2O.

Predicting RNA secondary structure. RNA Structure Program version 4.1 (http://rna.urmc.rochester.edu/rnastructure.html) was used to predict the secondary structures of A10 aptamer, A10-3, and A10 aptamer–siRNA chimera derivatives (A10-Plk1 shown). The most stable structures with the lowest free energies for each RNA oligo were compared.

Cell culture. HeLa cells were maintained at 37 °C and 5% CO_2 in DMEM supplemented with 10% FBS. Prostate carcinoma cell lines LNCaP (ATCC no. CRL-1740) and PC-3 (ATCC no. CRL-1435) were grown in RPMI 1640 and Ham's F12-K medium respectively, supplemented with 10% FBS.

PSMA cell-surface expression. PSMA cell-surface expression was determined by flow cytometry and/or immunoblotting using antibodies specific to human PSMA. HeLa, PC-3 and LNCaP cells were trypsinized, washed three times in PBS, and counted using a hemocytometer. We resuspended 200,000 cells (1×10^6 cells/ml) in 500 μl of PBS and 4% FBS and incubated at 25 °C for 20 min. Cells were then pelleted and resuspended in 100 μl of PBS and 4% FBS containing 20 μg/ml of primary antibody against PSMA (anti-PSMA 3C6: Northwest Biotherapeutics) or 20 μg/ml of isotype-specific control antibody. After a 40 min incubation at 25 °C cells were washed three times with 500 μl of PBS and 4% FBS and incubated with a 1:500 dilution of secondary antibody (anti-mouse IgG-APC) in PBS and 4% FBS for 30 min at 25 °C. Cells were washed as detailed above, fixed with 400 μl of PBS and 1% formaldehyde, and analyzed by flow cytometry. For immunoblotting, HeLa, PC-3 and LNCaP cells were collected as described above. Cell pellets were resuspended in 1× RIPA

buffer (150 mM NaCl, 50 mM Tris-HCl pH 8.0, 1 mM EDTA, 1% NP-40) containing 1× protease and phosphatase inhibitor cocktails (Sigma) and incubated on ice for 20 min. Cells were then pelleted and 25 μg of total protein from the supernatants were resolved on a 7.5% SDS-PAGE gel. PSMA was detected using an antibody specific to human PSMA (anti-PSMA 1D11; Northwest Biotherapeutics).

Cell-surface binding of aptamer-siRNA chimeras. PC-3 or LNCaP cells were trypsinized, washed twice with 500 μl PBS, and fixed in 400 μl of FIX solution (PBS and 1% formaldehyde) for 20 min at 25 °C. After washing cells to remove any residual trace of formaldehyde, cell pellets were resuspended in 1× Binding Buffer (1× BB) (20 mM HEPES pH 7.4, 150 mM NaCl, 2 mM $CaCl_2$, 0.01% BSA) and incubated at 37 °C for 20 min. Cells were then pelleted and resuspended in 50 μl of 1× BB (prewarmed at 37 °C) containing either 400 nM FAM-G labeled A10 aptamer or 400 nM FAM-G labeled aptamer-siRNA chimeras. Due to the low incorporation efficiency of FAM-G during the transcription reaction, for comparison of A10-Plk1 and mutA10-Plk1 cell surface binding up to 10 μM of FAM-G labeled aptamer chimeras were used. Concentrations of FAM-G labeled aptamer and aptamer-siRNA chimeras for the relative affinity measurements varied from 0 to 4 μM. Cells were incubated with the RNA for 40 min at 37 °C, washed three times with 500 μl of 1× BB prewarmed at 37 °C, and finally resuspended in 400 μl of FIX solution prewarmed at 37 °C. Cells were then assayed using flow cytometry as detailed above and the relative cell surface binding affinities of the A10 aptamer and A10 aptamer–siRNA chimera derivatives were determined.

Cell-surface binding competition assays. LNCaP cells were prepared as detailed above for the cell-surface binding experiments. We used 4 μM of FAM-G labeled A10 aptamer or A10 aptamer–siRNA chimera derivatives to compete with either unlabeled A10 aptamer (concentration varied from 0 to 4 μM) in 1× BB prewarmed at 37 °C or 2 μg of anti-PSMA 3C6 antibody in PBS and 4% FBS. Cells were washed three times as detailed above, fixed in 400 μl of FIX (PBS + 1% formaldehyde), and analyzed by flow cytometry.

5-α-dihydrotestosterone (DHT) treatment. LNCaP cells were grown in RPMI 1640 medium containing 5% charcoal-stripped serum for 24 h before addition of 2 nM 5-α-dihydrotestosterone (DHT) (Sigma) in RPMI 1640 medium containing 5% charcoal-stripped FBS for 48 h. PSMA expression was assessed by immunoblotting as detailed above. PSMA cell surface expression was analyzed by flow cytometry as detailed above. Cell-surface binding of FAM-G labeled A10 aptamer and FAM-G labeled A10-CON, A10-Plk1, and mutA10-Plk1 aptamer chimeras was done as detailed above using 40 μM of FAM-G labeled RNA.

Gene silencing assay. For siRNAs, (day 1) PC-3 and LNCaP cells were seeded in 6-well plates at 60% confluency. Cells were transfected with either 200 nM or 400 nM siRNA on day 2 and 4 using Superfect Reagent (Qiagen) following manufacturer's recommendations. Cells were collected on day 5 for analysis. For A10 aptamer and A10 aptamer–siRNA chimeras, (Day 1) PC-3 and LNCaP cells were seeded in 6-well plates at 60% confluency. Cells were treated with 400 nM A10 aptamer or A10 aptamer–siRNA chimeras on day 2 and 4. Cells were collected on day 5 for analysis.

Gene silencing was assessed by either quantitative RT-PCR (qRT-PCR) or flow cytometry and immunoblotting using antibodies specific to human *PLK1* (Zymed) and human *BCL2* (Zymed), respectively. Real-time PCR was performed on mRNA (50 ng) from LNCaP cells treated with the various siRNAs or chimeras using iScript One-Step RT-PCR Kit with SYBR Green (Biorad) with a Biorad iCycler. All reactions were done in a 50-μl volume in triplicate. Primers for human *GAPDH*, *PLK1* and *BCL2* are: *GAPDH* forward: 5′-TCGCTCTCTG CTCCTCCTGTTC-3′; *GAPDH* reverse: 5′-CGCCCAATACGACCAAATCC-3′; *PLK1* forward: 5′-GACAAGTACGGCCTTGGGTA-3′; *PLK1* reverse: 5′-GTGCC GTCACGCTCTATGTA-3′; *BCL2* forward: 5′-ATGTGTGTGGAGAGCGTCAA-3′; *BCL2* reverse: 5′-ACAGTTCCACAAAGGCATCC-3′. PCR parameters were as follows: 50 °C for 30 min, 5 min of *Taq* activation at 95 °C, followed by 45 cycles of PCR at 95 °C × 30 s, 57 °C × 30 s, 72 °C × 30 s. Standard curves were generated and the relative amount of target gene mRNA was normalized to *GAPDH* mRNA. Specificity was verified by melt curve analysis and agarose gel electrophoresis. For flow cytometry, PC-3 and LNCaP cells were trypsinized, washed three times in PBS and counted using a hemocytometer. We resuspended 200,000 cells (5 × 10^5 cells/ml) in 400 μl ofPERM/FIX buffer (Pharmingen) and incubated at 25 °C for 20 min. Cells were then pelleted and washed three times with 1× Perm/Wash buffer (Pharmingen). Cells were then resuspended in 50 μl 1× Perm/Wash buffer containing 20 μg/ml of primary antibody against either human *PLK1*, or human *BCL2*, or 20 μg/ml of isotype-specific control antibody. After 40 min incubation at 25 °C, cells were washed three times with 500 μl 1× Perm/Wash buffer and incubated with a 1:500 dilution of secondary antibody (anti-mouse IgG-APC) in 1× Perm/Wash for 30 min at 25 °C. Cells were washed as detailed above and analyzed by flow cytometry. For immunoblotting, LNCaP cells were transfected with control siRNA, or siRNAs to either *PLK1* or *BCL2* as described above. Cells were trypsinized, washed in PBS, and cell pellets were resuspended in 1× RIPA buffer and incubated on ice for 20 min. Cells were then pelleted and 50 μg of total protein from the supernatants were resolved on either 8.5% SDS-PAGE gel for *PLK1* or a 15% SDS-PAGE gel for *BCL2*. *PLK1* was detected using anantibody specific to human *PLK1* (Zymed). *BCL2* was detected using an antibody specific to human *BCL2* (Dykocytomation).

Proliferation (DNA synthesis) assay. PC-3 and LNCaP cells previously treated with siRNAs or aptamer-siRNA chimeras as detailed above, were trypsinized and seeded in 12-well plates at ~20,000 cells/well. Cells were then forced into a G1/S block by addition of 0.5 μM hydroxy urea (HU). After 21 h cells were released from the HU block by addition of medium lacking HU and incubated with medium containing ^{3}H-thymidine (1μ Ci/ml medium) to monitor DNA synthesis. After 24 h incubation in the presence of medium containing ^{3}H-thymidine, cells were washed twice with PBS, washed once with 5% wt/vol trichloroacetic acid (TCA) (VWR), collected in 0.5 ml of 0.5N NaOH (VWR) and placed in scintillation vials for measurement of ^{3}H-thymidine incorporation.

Active caspase 3 assay. PC-3 or LNCaP cells were either transfected with siRNAs to *PLK1* or *BCL2* or treated with A10 aptamer–siRNA chimeras as described above. Cells were also treated with medium containing 100 μM cisplatin for 30 h as a positive control for apoptosis. Cells were then fixed and stained for active caspase 3 using a PE-conjugated antibody specific to cleaved caspase 3 as specified in manufacturer's protocol (Pharmingen). Flow cytometric analysis was used to quantify percentage PE positive cells as a measure of apoptosis.

Dicer siRNA. HeLa cells were seeded in 6-well plates at 200,000 cells per well. After 24 h, cells were transfected with either 400 nM of control siRNA or an siRNA against human Dicer using Superfect Reagent as described above. Cells were then collected and processed for flow cytometric analysis using an antibody specific for human Dicer (IMX-5162; IMGENEX) as described above for analysis of *PLK1* and *BCL2* by flow cytometry.

Enzyme-linked immunosorbent assay (ELISA). HeLa cells were seeded in 6-well plates at 200,000 cells per well. After 24 h, cells were transfected with either 400 nM of control, nonsilencing siRNA or an siRNA against human dicer using Superfect Reagent as described above. Cells were then collected and lysed in 1× RIPA buffer containing 1× protease and phosphatase inhibitor cocktail (Sigma) for 20 min on ice. 100 μl of cell lysates were then added to each ELISA 96-well plate and incubated at 25 °C for 24 h. Wells were washed three times with 300 μl of 1× RIPA and incubated with 100 μl of 1:200 dilution of primary antibody to human Dicer in 1× RIPA for 2 h. Wells were washed as above, and incubated with 100 μl of 1:200 dilution of secondary anti-rabbit IgG-HRP antibody in 1× RIPA for 1 h. Wells were washed as above before addition of 100 μl of TMB substrate solution (PBL Biomedical Laboratories). After 20 min 50 μl of 1M H_2SO_4 (Stop Solution) was added to each well and OD_{450}–OD_{540} was determined using a plate reader.

***In vivo* dicer assay.** LNCaP cells were seeded in 6-well plates at 200,000 cells per well. After 24 h, cells were cotransfected with either 400 nM of control siRNA, 400 nM of *PLK1* siRNA, 400 nM A10 aptamer, or 400 nM of A10 aptamer–siRNA chimeras alone or with an siRNA to human Dicer, using Superfect Transfection Reagent as described above. Cells were then collected and processed for flow cytometric analysis using an antibody specific for human *PLK1* as described above.

***In vitro* dicer assay.** 1–2 μg of A10 aptamer or A10 aptamer–siRNA chimeras were digested using recombinant dicer enzyme following manufacturer's recommendations (Recombinant Human Turbo Dicer Kit; GTS)[35]. ssA10-CON and ssA10-Plk1 correspond to the aptamer-siRNA chimeras without the complementary antisense siRNA strand. Digests were then resolved on a 15% nondenaturing PAGE gel and stained with ethidium bromide before visualization using the GEL.DOCXR (BioRad) gel camera. Alternatively, 1–2 μg of A10 aptamer or A10 aptamer–siRNA chimera sense strands were annealed to ^{32}P-end-labeled complementary antisense siRNAs (probe). The siRNAs were end-labeled using T4 polynucleotide kinase (NEB) following manufacturer's recommendations. The antisense siRNAs were not complementary to the A10 aptamer. A10 or the annealed chimeras (A10-CON or A10-Plk1) were incubated with or without Dicer enzyme and subsequently resolved on a 15% nondenaturing PAGE gel as described above. The gel was dried and exposed toBioMAX MR film (Kodak) for 5 min.

5′ RACE analysis. mRNA (250 μg) from LNCaP cells treated with different siRNAs and chimeras was ligated to GeneRacer adaptor (Invitrogen) without prior treatment. Ligated RNA was reverse transcribed using gene specific primer (GSP(Plk1)-Rev1: 5′-GAATCCTACGACGTGCTGGT-3′). To detect cleavage products, PCR was performed using primers complementary to the RNA adaptor (GR5′ primer: 5′-CTCTAGAGCGACTGGAGCACGAGGACA CTA-3′) and gene-specific primer (GSP(Plk1)-Rev2: 5′-GCTGCGGTGAATGG ATATTT-3′). Amplification products were resolved by agarose gel electrophoresis and visualized by ethidium bromide staining. The identity of the specific PCR products was confirmed by sequencing of the excised bands.

Interferon assay. Secreted IFN-β from treated and untreated PC-3 and LNCaP cells was detected using a human interferon beta ELISA kit following manufacturer's recommendations (PBL Biomedical Laboratories). Briefly, cells were seeded at 200,000 cells/well in 6-well plates. Twenty-four hours later, cells were either transfected with a mixture of Superfect Transfection Reagent (Qiagen) plus varying amounts of Poly(I:C) (2.5, 5, 10, 15 μg/ml) as a positive control for Interferon beta, or with a mixture of Superfect Transfection Reagent and either con siRNAs or siRNAs to *PLK1* or *BCL2* (200 nm or 400 nm). In addition, cells were treated with 400 nM each of A10 aptamer and A10 aptamer–siRNA chimeras as described above. We added, 48 h after the various treatments, 100 μl of supernatant from each treatment group to a well of a 96-well plate and incubated at 25 °C for 24 h. Presence of INF-beta in the supernatants was detected using an antibody specific to human INF-beta following manufacturer's recommendations.

***In vivo* experiments.** Athymic nude mice (nu/nu) were obtained from the Cancer Center Isolation Facility (CCIF) at Duke University and maintained in a sterile environment according to guidelines established by the US Department of Agriculture and the American Association for Accreditation of Laboratory Animal Care (AAALAC). This project was approved by the Institutional Animal Care and Utilization Committee (IAUCUC) of Duke University. Athymic mice were inoculated with either 5×10^6 (in 100 μl of 50% Matrigel) *in vitro* propagated PC-3 or LNCaP cells subcutaneously injected into each flank. Approximately 32 non-necrotic tumors for each tumor type, which exceeded 1 cm in diameter, were randomly divided into four groups of eight mice per treatment group as follows: group 1, no treatment (DPBS); group 2, treated with A10-CON chimera (200 pmols/injection × 10); group 3, treated with A10-Plk1 chimera (200 pmols/injection × 10); group 4, treated with mut-A10-Plk1 chimera (200 pmols/injection X 10). Compounds were injected intratumorally in 75-μl volumes every other day for a total of 20 d. Day 0 marks the first day of injection. The small volume injections are small enough to preclude the compounds being forced inside the cells due to a nonspecific high-pressure injection. Tumors were measured every 3 d with calipers in three dimensions. The following formula was used to calculate tumor volume: V_T = WXLXH)X0.5236 (W, the shortest dimension; L, the longest dimension). The growth curves are plotted as the means tumor volume ± s.e.m. The animals were killed 3 d after the last treatment when the tumors were excised and formalin fixed for immunohistochemistry. Slides of serial sections were stained with hematoxylin and eosin (H&E).

Statistical analysis. Statistical analysis was conducted using a one-way ANOVA. A $P \leq 0.05$ was considered to indicate a significant difference. In addition to a one-way ANOVA, two-tailed unpaired *t*-tests were conducted to compare each treatment group to every other. For tumors expressing PSMA, group 3 (A10-Plk1) was significantly different from group 1 (DPBS), group 2 (A10-CON) and group 4 (mutA10-Plk1), $P < 0.01$, on days 12, 15, 18 and 21. Group 2 (A10-CON) and group 4 (mutA10-Plk1) were not significantly different from the DPBS control group, $P > 0.05$, at any point during the treatment. For PSMA negative tumors, there was no significant difference between the groups.

Intratumoral injection analysis. FITC-labeled chimera molecule solution was prepared as described above. Evans blue-labeled albumin solution was prepared by mixing albumin and Evans blue in 0.9% saline[36,37]. Their final concentrations were 0.1% and 0.04%, respectively. We then injected 100 μl of solution. After the injection, the tumor was harvested and sectioned into 600-μm slices with a Vibratome (Model 3000; Technical Products International). For the intratumoral injection of Evans blue-labeled albumin solution, tumor slices were mounted on microscope slides and scanned into a computer with a Plustek Optic Pro document scanner (Model 12000P). For the intratumoral injection of FITC-labeled A10-Plk1 reagent, tumor slices were imaged using a fluorescence lightbox (LT9MACROIMSYS; Lightools Research). Images were collected with a color CCD camera and analyzed using theImage Pro Plus v.4.0 software (Media Cybernetics, Inc). $n = 4$ tumors were analyzed of which two are shown.

Note: Supplementary information is available on the Nature Biotechnology website.

ACKNOWLEDGMENTS

We thank John Madden and Johannes Vieweg for useful discussions and Mariano Garcia-Blanco and Joseph R. Nevins for useful reagents. B.A.S., E.G., R.E.R., Y.W., K.D.V. and P.H.G. are supported by the National Institutes of Health (NIH). E.R.A. is supported by a postdoctoral training grant from Susan G. Komen Breast Cancer Foundation. J.O.M. is supported by an NIH postdoctoral training grant (5T32CA00911-28). This work was supported by NIH grants 2P01GM059299 and 1U54CA119313 to B.A.S.

AUTHOR CONTRIBUTIONS

J.O.M. II designed, performed research and wrote manuscript; E.R.A. provided expertise, performed research, and analyzed data; Y.W. performed research; K.D.V. provided expertise; R.E.R. provided useful reagents; E.G. provided useful discussions and analytic tools; B.A.S. suggested chimera idea and provided useful discussions; P.H.G. designed, coordinated and performed research, analyzed data, wrote manuscript.

COMPETING INTERESTS STATEMENT

The authors declare that they have no competing financial interests.

Published online at http://www.nature.com/naturebiotechnology/
Reprints and permissions information is available online at http://npg.nature.com/reprintsandpermissions/

1. Fire, A. *et al.* Potent and specific genetic interference by double-stranded RNA in *Caenorhabditis elegans*. *Nature* **391**, 806–811 (1998).
2. Elbashir, S.M. *et al.* Duplexes of 21-nucleotide RNAs mediate RNA interference in cultured mammalian cells. *Nature* **411**, 494–498 (2001).
3. Yano, J. *et al.* Antitumor activity of small interfering RNA/cationic liposome complex in mouse models of cancer. *Clin. Cancer Res.* **10**, 7721–7726 (2004).
4. Fountaine, T.M., Wood, M.J. & Wade-Martins, R. Delivering RNA interference to the mammalian brain. *Curr. Gene Ther.* **5**, 399–410 (2005).
5. Devroe, E. & Silver, P.A. Therapeutic potential of retroviral RNAi vectors. *Expert Opin. Biol. Ther.* **4**, 319–327 (2004).
6. Anderson, J., Banerjea, A., Planelles, V. & Akkina, R. Potent suppression of HIV type 1 infection by a short hairpin anti-CXCR4 siRNA. *AIDS Res. Hum. Retroviruses* **19**, 699–706 (2003).
7. Lewis, D.L. & Wolff, J.A. Delivery of siRNA and siRNA expression constructs to adult mammals by hydrodynamic intravascular injection. *Methods Enzymol.* **392**, 336–350 (2005).
8. Schiffelers, R.M. *et al.* Cancer siRNA therapy by tumor selective delivery with ligand-targeted sterically stabilized nanoparticle. *Nucleic Acids Res.* **32**, e149 (2004).
9. Urban-Klein, B. *et al.* RNAi-mediated gene-targeting through systemic application of polyethylenimine (PEI)-complexed siRNA in vivo. *Gene Ther.* **12**, 461–466 (2005).
10. Soutschek, J. *et al.* Therapeutic silencing of an endogenous gene by systemic administration of modified siRNAs. *Nature* **432**, 173–178 (2004).

11. Lorenz, C. *et al.* Steroid and lipid conjugates of siRNAs to enhance cellular uptake and gene silencing in liver cells. *Bioorg. Med. Chem. Lett.* **14**, 4975–4977 (2004).
12. Minakuchi, Y. *et al.* Atelocollagen-mediated synthetic small interfering RNA delivery for effective gene silencing *in vitro* and *in vivo*. *Nucleic Acids Res.* **32**, e109 (2004).
13. Takeshita, F. *et al.* Efficient delivery of small interfering RNA to bone-metastatic tumors by using atelocollagen *in vivo*. *Proc. Natl. Acad. Sci. USA* **102**, 12177–12182 (2005).
14. Song, E. *et al.* Antibody mediated *in vivo* delivery of small interfering RNAs via cell-surface receptors. *Nat. Biotechnol.* **23**, 709–717 (2005).
15. Hu-lieskovan, S., Heidel, J.D., Bartlett, D.W., Davis, M.E. & Triche, T.J. Sequence-specific knockdown of EWS-FLI1 by targeted, noviral delivery of small interfering RNA inhibits tumor growth in a murine model of metastatic Ewing's sarcoma. *Cancer Res.* **65**, 8984–8992 (2005).
16. Lupold, S.E., Hicke, B.J., Lin, Y. & Coffey, D.S. Identification and characterization of nuclease-stabilized RNA molecules that bind human prostate cancer cells via the prostate-specific membrane antigen. *Cancer Res.* **62**, 4029–4033 (2002).
17. Reagan-Shaw, S. & Ahmad, N. Silencing of polo-like kinase (Plk) 1 via siRNA causes induction of apoptosis and impairment of mitosis machinery in human prostate cancer cells: implications for the treatment of prostate cancer. *FASEB J.* **19**, 611–613 (2005).
18. Takai, N. *et al.* Polo-like kinases (Plks) and cancer. *Oncogene* **24**, 287–291 (2005).
19. Eckerdt, F., Yuan, J. & Strebhardt, K. Polo-like kinases and oncogenesis. *Oncogene* **24**, 267–276 (2005).
20. Cory, S. & Adams, J.M. Killing cancer cells by flipping the Bcl-2/Bax switch. *Cancer Cell* **8**, 5–6 (2005).
21. Pestourie, C., Tavitian, B. & Duconge, F. Aptamers against extracellular targets for in vivo applications. *Biochimie* **87**, 921–930 (2005).
22. Nimjee, S.M., Rusconi, C.P. & Sullenger, B.A. Aptamers: an emerging class of therapeutics. *Annu. Rev. Med.* **56**, 555–583 (2005).
23. Israeli, R.S. *et al.* Expression of the prostate-specific membrane antigen. *Cancer Res.* **54**, 1807–1811 (1994).
24. Doi, N. *et al.* Short-interfering-RNA-mediated gene silencing in mammalian cells requires Dicer and eIF2C translation initiation factors. *Curr. Biol.* **13**, 41–46 (2003).
25. Murchison, E.P., Partridge, J.F., Tam, O.H., Cheloufi, S. & Hannon, G.J. Characterization of Dicer-deficient murine embryonic stem cells. *Proc. Natl. Acad. Sci. USA* **102**, 12135–12140 (2005).
26. Kim, D.H. *et al.* Synthetic dsRNA Dicer substrates enhance RNAi potency and efficacy. *Nat. Biotechnol.* **23**, 222–226 (2005).
27. Sledz, C.A. *et al.* Activation of the interferon system by short-interfering RNAs. *Nat. Cell Biol.* **5**, 834–839 (2003).
28. Kariko, K., Bhuyan, P., Capodici, J. & Weissman, D. Small interfering RNAs mediate sequence-independent gene suppression and induce immune activation by signaling through toll-like receptor 3. *J. Immunol.* **172**, 6545–6549 (2004).
29. Allerson, C.R. *et al.* Fully 2'-modified oligonucleotide duplexes with improved *in vitro* potency and stability compared to unmodified small interfering RNA. *J. Med. Chem.* **48**, 901–904 (2005).
30. Layzer, J.M. *et al. In vivo* activity of nuclease-resistant siRNAs. *RNA* **10**, 766–771 (2004).
31. Cui, Y., Ulrich, H. & Hess, G.P. Selection of 2'-fluoro-modified RNA aptamers for alleviation of cocaine and MK-801 inhibition of the nicotinic acetylcholine receptor. *J. Membr. Biol.* **202**, 137–149 (2004).
32. Park, K.W. Protamine and protamine reactions. *Int. Anesthesiol. Clin.* **42**, 135–145 (2004).
33. Shepherd, G.M. Hypersensitivity reactions to drugs: evaluation and management. *Mt. Sinai J. Med.* **70**, 113–125 (2003).
34. Padilla, R. & Sousa, R. Efficient synthesis of nucleic acids heavily modified with non-canonical ribose 2'-groups using a mutantT7 RNA polymerase (RNAP). *Nucleic Acids Res.* **27**, 1561–1563 (1999).
35. Myers, J.W., Jones, J.T., Meyer, T. & Ferrell, J.E., Jr. Recombinant Dicer efficiently converts large dsRNAs into siRNAs suitable for gene silencing. *Nat. Biotechnol.* **21**, 324–328 (2003).
36. Wang, Y., Wang, H., Li, C.Y. & Yuan, F. Effects of rate, volume, and dose of intratumoral infusion on virus dissemination in local gene delivery. *Mol. Cancer Ther.* **5**, 362–366 (2006).
37. McGuire, S. & Yuan, F. Quantitative analysis of intratumoral infusion of color molecules. *Am. J. Physiol. Heart Circ. Physiol.* **281**, H715–H721 (2001).